Effects of Hydration, Ion Release, and Excluded Volume on the Melting of Triplex and Duplex DNA†

Charles H. Spink‡ and Jonathan B. Chaires*,§

Department of Chemistry, State University of New York, Cortland, New York 13045, and Department of Biochemistry, University of Mississippi Medical Center, 2500 North State Street, Jackson, Mississippi 39216-4505

Received August 20, 1998; Revised Manuscript Received November 9, 1998

ABSTRACT: The stability of DNA duplex and triplex structures not only depends on molecular forces such as base pairing or tripling or electrostatic interactions but also is sensitive to its aqueous environment. This paper presents data on the melting of *Escherichia coli* and poly(dA)·poly(dT) duplex DNA and on the poly(dT)·poly(dA)·poly(dT) triplex in a variety of media to assess the contributions from the osmotic status and salt content of the media. The effects of volume exclusion on the stability of the DNA structures are also studied. From thermal transition measurements in the presence of low-molecular weight osmotic stressors, the number of water molecules released upon melting is found to be four waters per base pair for duplex melting and one water for the conversion of triplex to single-strand and duplex. The effects of Na^+ counterion binding are also determined in ethylene glycol solutions so that the variation of counterion binding with water activity is evaluated. The data show that there is a modest decrease in the extent of counterion binding for both duplex and triplex as water activity decreases. Finally, using larger polyethylene glycol cosolutes, the effects on melting of volume exclusion by the solutes are assessed, and the results correlated with simple geometric models for the excluded volume. These results point out that DNA stability is sensitive to important conditions in the environment of the duplex or triplex, and thus, conformation and reactivity can be influenced by these solution conditions.

The stability of duplex and triplex polynucleotides is dependent upon a number of important nonbonding interactions. Hydrogen bonding and base stacking interactions between base pairs and repulsive electrostatic charges play major roles in the thermodynamic stability of DNA (*1*−*5*). There is also evidence that water molecules bound at specific and/or nonspecific sites along the DNA chain influence the stability of the duplex nucleotide strands (*6*−*10*). Determination of the effects of this hydration on the chemical and physical properties of DNA thus depends on evaluation of the quantity of water bound, and how the water content changes when DNA undergoes physical or chemical change.

Evaluation of the amount water specifically bound to DNA has been attempted by several approaches, and the results are dependent upon the experimental methodology used (*6*, *8*, *9*). Early studies on binding isotherms of water to solid polynucleotides revealed that up to a relative humidity of about 75%, the BET equation describes the adsorption behavior with about two water molecules per nucleotide binding as a monolayer (*11*). This primary monolayer was ascribed to hydration of phosphate sites, and was found to be about the same for RNA, DNA, and single-stranded poly(dA). As the relative humidity approaches 100%, the level of water binding increases to between 15 and 20 waters per nucleotide depending on the polynucleotide. Infrared and nuclear magnetic resonance spectroscopy have been used to identify sites where water molecules interact with DNA, and these studies confirm that the first water molecules adsorbed on solid DNA as the relative humidity increases are in the sugar−phosphate region (*12*, *13*). NMR studies are also useful in providing information about the lifetimes of water molecules associated with particular sites in DNA triplexes (*14*). The minor groove in DNA with A_nT_n tracts shows water that is bound rather tightly as reflected in long lifetimes for exchange from these sites (*15*). The wider grooves associated with RNA sequences indicate shorter lifetimes, a reflection of weak hydration in the grooves of the A-type structure (*16*).

Useful information about bound water in polynucleotides has been obtained from refinement of the crystal structures of small oligonucleotides (*7*, *8*). Very specific ordered hydration sites have been found for decamers of B-type DNA in the first hydration shell (*17*). An upper limit of about five water molecules per base pair in the vicinity of the bases, along with four waters per phosphate and two waters in the ribose sugar region, has been identified as specifically bound water. These numbers add up to about 17 ordered water molecules per base pair that are bound in the duplex form of DNA. Interestingly, these data indicate that guanine and adenine show the same extent of hydration, as do cytosine and thymine, suggesting that hydration numbers should not depend on sequence in the DNA chain.

Direct thermodynamic evidence for hydration of DNA has been presented on the basis of compressibility and molar volume measurements (*18*−*20*). These studies have inferred

† This work was supported by a grant from the National Cancer Institute (CA35635).

* To whom correspondence should be addressed.

‡ State University of New York.

§ University of Mississippi Medical Center.

10.1021/bi9820154 CCC: $18.00
Published on Web 12/11/1998

the presence of bound water that is thermodynamically different from bulk water. This bound water can be released when specific ligands bind to DNA producing significant molar volume and entropic changes as the water is released during the binding event (*19*, *20*). The use of osmotic stressing experiments, a method that induces water activity changes by addition of solutes which do not interact with the polynucleotide, can also show the influence that bound water has on equilibria involving DNA (*21*−*23*). A recent paper by Vossen et al. (*23*) describes how hydration affects the binding of the *Escherichia coli* cyclic AMP receptor to DNA. Formation of the complex between the receptor and its regulatory site on DNA releases about 79 water molecules, and using arguments about the area occupied per water molecule, it was found that about 700 Å^2 of the surface area become inaccessible upon formation of the complex. This area agreed well with areas calculated on the basis of crystal structures of the CAP−DNA complex.

These latter studies of hydration use the linkage concepts developed by Wyman (*24*, *25*), later formulated into osmotic stress methods by Parsegian (*21*, *26*). Small neutral cosolutes in the presence of macromolecules have been shown to be excluded from the immediate vicinity of the protein or polynucleotide, leading to preferential hydration of the surfaces of the macromolecule (*27*−*31*). Thus, if there is a significant number of water molecules associated with the macromolecule surface, equilibria that involve changes in surface exposure become sensitive to changes in the water activity induced by the cosolutes. Thus, study of the dependence of the equilibrium constant on water activity provides a direct route for determining the changes in the number of water molecules involved in the equilibrium reaction (*21*, *32*, *33*).

Zimmerberg and Parsegian (*64*) have shown that in addition to the effects that cosolutes have on water activity, the size of the perturbant can be an important factor in the response of a protein to its environment. Polyethylene glycols (PEGs) of varying size affect conductance through alamethicin channels through dehydration of the protein channel by osmotic stress (lowered water activity). But, in addition, it was observed that smaller PEGs actually penetrate the channels, and thus cut conductance through blockage of movement of anions through the channel. As size increases, the obstruction diminishes since the larger cosolutes cannot penetrate the interior of the channel. These size effects point out the need to use cosolutes with a wide range of molecular weights to separate osmotic from geometric effects of the solutes (*65*).

The addition of cosolutes, which alter water activity, to the environment of the DNA should produce significant effects on the free energy of melting of triplex or duplex if there are changes in the number of bound waters as melting occurs. This paper addresses the question of how much influence this thermodynamically significant hydration has on the thermal denaturation of several duplex and triplex DNA samples. The intent is to evaluate the role of changes in water activity and cosolute volume on the thermodynamics of melting of polynucleotide chains. There have been several reports of the melting of DNA in the presence of cosolutes. Although there was no quantitative analysis of the results, a study of the thermal transitions in the presence of PEGs and several polysaccharides with varying molecular weights showed that smaller cosolutes destabilize the duplex, while larger solutes raised the temperature of melting (*34*). In another study, the effects of increasing concentrations of PEG again showed stabilization of duplex RNA, and the results were interpreted as an effect of excluded volume on the activity coefficients of the single- and double-stranded polynucleotide (*35*). This alternative way of describing in detail the effects neutral solutes have on macromolecular equilibria is to treat the changes as a consequence of thermodynamic nonideality induced by molecular crowding (*36*−*38*). In this treatment, it is shown that there is an apparent equivalence of preferential hydration in the presence of solutes, such as glycerol or sucrose, with simple nonideality of the components in equilibrium due to the effect that the cosolutes have on the available molecular space to the macromolecular components (*36*). The effects of crowding are particularly evident for larger cosolute molecules, such as the polyethylene glycols (PEG), leading to significantly increased effects on equilibria involving proteins (*23*), and on aggregation reactions of DNA (*39*).

We have reported earlier the effects of PEG cosolutes on the melting behavior of duplex poly(dA)·poly(dT) and triplex poly(dT)·poly(dA)·poly(dT), which showed a selective stabilization of triplex relative to duplex as the size of the solute increased (*40*). In this paper, we extend our previous study by showing the effects of a variety of cosolutes on the thermal melting of double- and triple-helical DNA. The data indicate that for the smaller solutes there is a general destabilization of the associated strands of DNA, while for larger PEG cosolutes the duplex and particularly the triplex forms are markedly stabilized. We use the concepts relating to changes in water activity and, for the larger solutes, the excluded volume effect to explain the changes in DNA stability in the presence of the cosolutes. The correlated changes in bound sodium ions upon melting of the duplex and triplex DNA are also determined.

MATERIALS AND METHODS

Materials. Several different DNA samples were used in this study. *E. coli* DNA was obtained from Sigma Chemical Co. (St. Louis, MO) and was sheared by sonication in a horn sonication cell to reduce the size of the duplex to about 200 base pairs. The sheared sample was extensively dialized against BPE buffer [0.01 M sodium phosphate and 0.001 M disodium ethylenediaminetetraacetic acid (pH 7.0)] before use. Triplex poly(dT)·poly(dA)·poly(dT) was prepared by mixing poly(dT) with poly(dA)·poly(dT) (both from Pharmacia Co., Piscataway, NJ), heating to 90 °C, and slowly cooling to room temperature. The triplex samples were dialyzed against CNE buffer, consisting of 10 mM sodium cacodylate, 0.1 mM disodium EDTA, and 300 mM NaCl (pH 7.4). In some of the measurements on triplex melting, the NaCl content was reduced to 0.21 and 0.14 M in the buffer. The low-molecular weight cosolutes were reagent grade, and the polyethylene glycols were from Sigma Chemical Co. and had nominal molecular weights of 400 (PEG 04), 1000 (PEG 1), 3400 (PEG 3), and 8000 (PEG 8). All cosolutes were dissolved in the appropriate buffer for combination with DNA solutions.

Physical Measurements. In general, solutions for the physical measurements reported below were prepared by

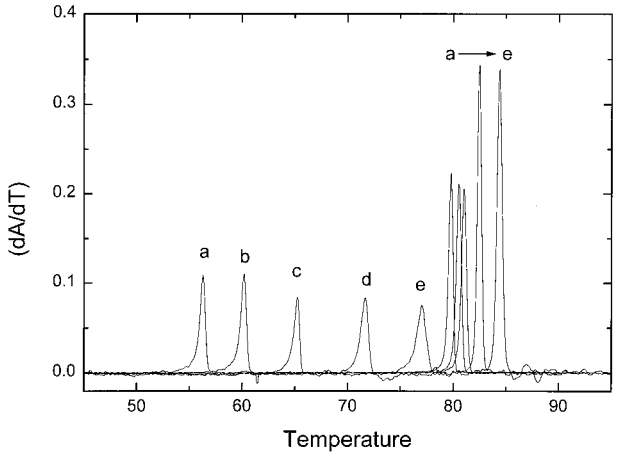

FIGURE 1: Derivative melting curves for poly(dT)·poly(dA)·poly(dT) in solutions containing PEG 3400: (a) CNE buffer and (b) 5, (c) 10, (d) 15, and (e) 20 wt %/volume PEG. The lower temperature peaks are for triplex and the higher for duplex.

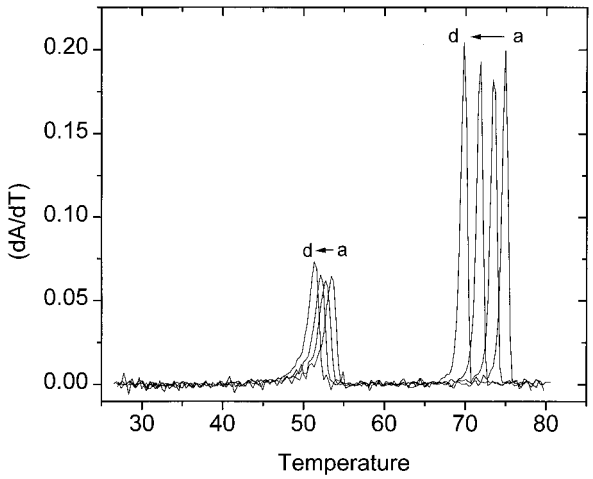

FIGURE 2: Derivative melting curves for poly(dT)·poly(dA)·poly(dT) in solutions containing ethylene glycol: (a) 5, (b) 10, (c) 15, and (d) 20 wt %/volume ethylene glycol.

mixing the DNA and cosolute solutions each dissolved in the same buffer medium. Thermal transitions of the DNA samples were measured by monitoring UV absorption at 260 nm, and using a programmed temperature scan (1 °C/min) with either a Carey 3E spectrophotometer or a Hewlett-Packard model 8452 diode array spectrophotometer. The osmotic pressures of the cosolute solutions in which all of the thermal melting transitions were studied were measured by vapor phase osmometry at room temperature, using a Wescor vapor pressure osmometer (model 5520). The measurements were calibrated using standard solutions of NaCl. In calculating of the water activity from osmotic pressure, we assumed that there is only small temperature dependence of the water activity between 25 and 80 °C, an observation that has been confirmed experimentally (*41*). Circular dichroism (CD) measurements were also taken on a number of the solutions studied. The data were obtained using a Jasco model 500 instrument, scans being run from 350 to 210 nm. The CD scans were run on solutions of DNA in the presence and absence of cosolutes, and in some cases after the melting transitions. Molar volumes of the solutes used were determined using 25 mL pycnometers over a range of concentrations from 0 to 20 wt % per volume of cosolute in buffer.

RESULTS

Effects of Low-Molecular Weight Cosolutes. Figures 1 and 2 show representative UV melting curves (plotted as the derivative of the absorbance with respect to temperature) for triplex poly(dT)·poly(dA)·poly(dT) in two different cosolute solutions. It is clear that the cosolutes affect the melting behavior in different ways, PEG 3400 causing an increase and ethylene glycol a decrease in T_m. Similar results were obtained for solutions of *E. coli* DNA under the same cosolute solutions. In Figure 3, we summarize the data for the variation of T_m with osmolality for the melting transitions of the DNA studied. The low-molecular weight cosolutes, such as ethylene glycol or glycerol, cause a depression of the melting temperature with increasing concentrations of the cosolute, while the larger PEG solutes generally yield an increase in T_m with increasing osmolality. This is true

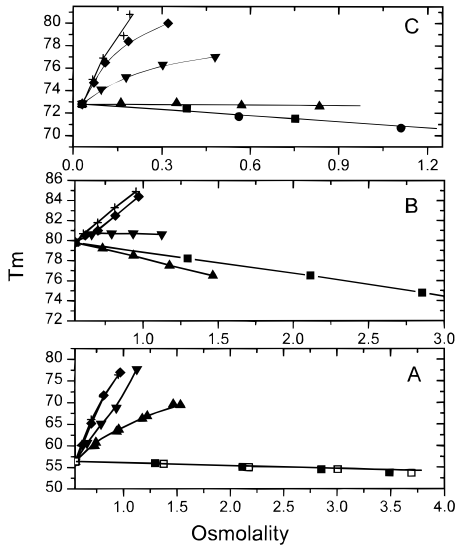

FIGURE 3: Melting temperatures at different osmolalities for (A) triplex poly(dT)·poly(dA)·poly(dT) DNA in solutions of cosolutes, (■ and □) ethylene glycol, (▲) PEG 400, (▼) PEG 1000, (◆) PEG 3400, and (+) PEG 8000, (B) duplex poly(dA)·poly(dT) DNA in solutions of cosolutes (symbols like those described for panel A), and (C) duplex *E. coli* DNA in solutions of cosolutes, (●) glycerol (other symbols like those described for panel A).

for both triplex and duplex melting transitions in poly(dT)·poly(dA)·poly(dT). The slopes for the smaller cosolutes seem to cluster near a common value, suggesting that water activity effects play a major role in the behavior of the DNA, so what follows is an analysis based on osmotic stressing methods using a wider variety of small cosolutes. The data for the larger solutes will be analyzed below using a consideration of the excluded volumes of the cosolutes.

The melting of DNA can be described in the presence of osmotic stressors by the following reaction:

$$\text{duplex} \leftrightarrows 2 \text{ single strands} + \Delta n_w H_2O + \Delta n_s S + \Delta n_{Na^+} Na^+ \quad (1)$$

where Δn_w, Δn_s, and Δn_{Na^+} are the changes in the number of waters, solute molecules, and sodium ions associated with

the melting of the duplex, respectively. A similar expression can be written for the melting of triplex DNA:

$$\text{triplex} \leftrightarrows \text{duplex} + \text{single strand} + \Delta n_w H_2O + \Delta n_s S + \Delta n_{Na^+} Na^+ \quad (2)$$

According to linkage concepts (*42*), changes in the equilibrium constants for the above reactions are dependent on any alterations of water activity and solute or ionic concentrations as determined by the following relationship:

$$d(\ln K) = \left[\frac{\partial(\ln K)}{\partial(\ln a_w)}\right] d(\ln a_w) + \left[\frac{\partial(\ln K)}{\partial(\ln a_s)}\right] d(\ln a_s) + \left[\frac{\partial(\ln K)}{\partial(\ln a_\pm)}\right] d(\ln a_\pm) \quad (3)$$

where a_i is the activity of either water, cosolute, or NaCl. It has been shown by Wyman (*24*) that

$$\frac{\partial(\ln K)}{\partial(\ln a_i)} = \Delta n_i \quad (4)$$

Thus,

$$\frac{d(\ln K)}{d(\ln a_w)} = \Delta n_w + \Delta n_s \left[\frac{d(\ln a_s)}{d(\ln a_w)}\right] + \Delta n_\pm \left[\frac{d(\ln a_\pm)}{d(\ln a_w)}\right] \quad (5)$$

If we now express the equilibrium constant in terms of the change in T_m with water activity, eq 5 becomes

$$-\frac{\Delta H^\circ}{R}\left[\frac{d(T_m^{-1})}{d(\ln a_w)}\right] = \Delta n_w + \Delta n_s \left[\frac{d(\ln a)}{d(\ln a_w)}\right] + \Delta n_\pm \left[\frac{d(\ln a_\pm)}{d(\ln a_w)}\right] \quad (6)$$

ΔH° is the enthalpy of melting of the duplex or triplex DNA. Equation 6 indicates that the slope of a plot of T_m^{-1} versus $\ln a_w$ is dependent on the change in the number of moles of water involved in the melting process, as well as contributions from the cosolute and salt as water activity changes. As will be discussed below, the last term in eq 6 relates to the release of sodium ion during melting. In the experiments designed to evaluate water binding, the ionic strength was almost constant (the dilution of the buffer with cosolute would change the ion concentrations a few percent, but the derivative term is small in magnitude). Also, as will be shown in the next section, $\Delta n_\pm$ is small, thus making the last term in eq 6 small. The cosolute term in eq 6 must now be considered.

Figure 4 shows plots of T_m^{-1} versus $\ln a_w$ for the low-molecular weight solutes and for the three DNA samples used. As mentioned above, the term $\Delta n_s[d(\ln a_s)/d(\ln a_w)]$ in eq 6 reflects any changes associated with preferential binding of the cosolute with DNA so that Δn_s would represent changes in the level of solute binding when the melting process occurs. For duplex DNA, the fact that the various solutes in Figure 4 all give the same slope within the experimental error would mean either that Δn_s is the same for all of the solutes (and the change in activity of the solute with the change in water activity is the same) or that Δn_s is

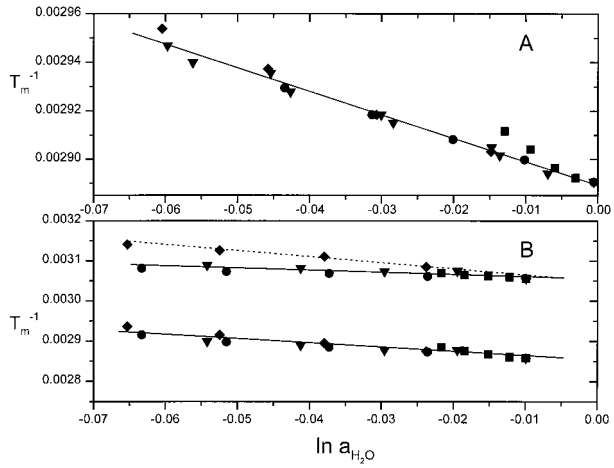

FIGURE 4: (A) Reciprocal temperature of melting for *E. coli* DNA vs the logarithm of water activity for small cosolutes: (●) glycerol, (■) sucrose, (◆) acetamide, and (▼) ethylene glycol. (B) Reciprocal temperature of melting of triplex poly(dT)·poly(dA)·poly(dT) (upper curves) and of duplex poly(dA)·poly(dT) (lower curves) vs the logarithm of water activity for small cosolutes: (●) glycerol, (■) sucrose, (◆) acetamide, and (▼) ethylene glycol.

very small, and thus, the slope of the T_m^{-1} versus $\ln a_w$ curve is determined largely by Δn_w instead. We prefer this latter interpretation, since it would seem unlikely that all of the cosolutes, whose structures are rather different, would have the same degree of preferential interaction with DNA. These same cosolutes were used in the study of binding of the CAP protein to DNA, and again the equilibrium constant of association was found to vary essentially the same for all solutes, suggesting that the origin of change was in the water activity, not a change in the degree of solute association (*23*). The binding of the drug netropsin to DNA was also found to be insensitive to the identity of cosolute when added to the reaction mixtures, and the binding changes upon addition of solute could be explained by water activity changes (*22*). Several studies involving the addition of these small cosolutes in protein−ligand binding systems also support the notion that the effects on binding are reflected through variation of water activity in the medium (*21*, *32*, *33*).

Examination of the data in Figure 4 shows that for the duplex melts either of *E. coli* or for poly(dA)·poly(dT) DNA, all of the points in each case fall on a common regression line, with only a few points outside of the 95% confidence limits. The slopes of the consensus lines are −0.00105 for poly(dA)·poly(dT) and −0.00111 for the *E. coli* DNA melts. The plots of T_m^{-1} versus $\ln a_w$ for triplex poly(dT)·poly(dA)·poly(dT) are not quite as consistent. Acetamide, although showing a negative slope, has a value that is significantly different from the three other solutes. It is not clear why the acetamide data show a slope different from the others, but as will be shown below, the slope difference has a relatively small effect on the calculated average value of Δn_w. Global regression for the data for ethylene glycol, glycerol, and sucrose yield a slope of −0.000562 for the triplex melt.

Before we proceed with the calculations of Δn_w using eq 6, one other issue needs to be considered. As pointed out by Vossen et al. (*23*), it is important to test whether the effects of cosolutes could be a result of dielectric constant alterations of the medium. If so, then changes in the melting temper-

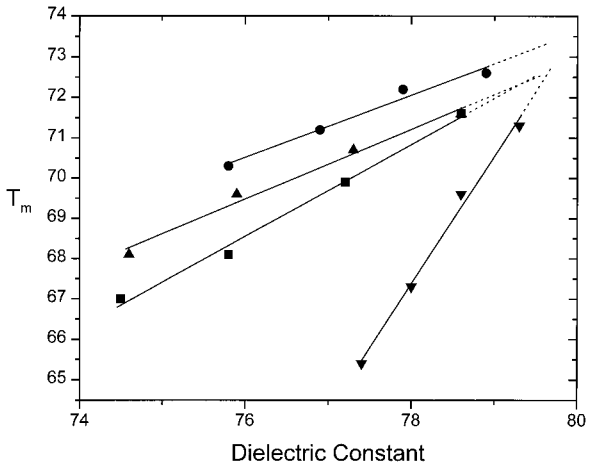

FIGURE 5: Variation of the melting temperature of *E. coli* DNA as a function of dielectric constant for solutions of (●) sucrose, (▲) glycerol, (■) ethylene glycol, and (▼) acetamide.

atures could be a reflection of effects on the electrostatic charge density along the DNA chain, which could also alter the chemical potential of the duplex. From the dielectric increment data of Cohn and Edsall (*43*), the dielectric constants of several of the media used above can be calculated. Figure 5 shows the relationships between T_m^{-1} and dielectric constants for four of the solutes used. If the dissociation constant for strand separation scaled with the dielectric constant of the solution, then the slopes of curves in Figure 5 should all fall on a common line. However, the curves clearly show that there are significant differences in the slopes for all four solutes, a reflection that T_m, and thus the equilibrium constant for the melting of the duplex, does not scale with the dielectric constants. This result supports the idea that the major effect of cosolute on the melting transitions is caused by changes in water activity.

If the presumption that the low-molecular weight cosolutes are influencing DNA melting only through water activity changes, with the last two terms in eq 6 considered insignificant, then the slopes of T_m^{-1} versus ln a_w allow calculation of Δn_w, the change in the number of moles of water per base pair upon melting of the duplex or triplex chains. The calculation requires a value for $\Delta H°$ for duplex and triplex melting. Unfortunately, the values of $\Delta H°$ seem to depend on the source of the DNA, particularly for the poly(dA)·poly(dT) melt (*44*). For the triplex transition, there are several values for the TAT triplet: 2.33 kcal/mol of base triplet from the melting of a decamer (*45*) and 3.36 kcal/mol of base triplet based on calorimetric measurement of melting of poly(dT)·poly(dA)·poly(dT) (*46*). Recent calorimetric values for duplex poly(dA)·poly(dT) melting are 6.87 kcal/mol of base pair (*46*) and 6.0 kcal/mol for the decamer (*45*). We choose the values of Haq (*46*) because our source (Pharmacia) of the duplex and methods of preparation of the triplex DNA are the same. In Table 1, we summarize the numbers (Δn_w) for the individual solutes, and also show the number obtained for the global fit to the combined data sets, as shown in Figure 4. The value for sucrose in Table 1 is about twice the values for the other solutes when taking the slope from the individual data set. This could indicate a small, specific solute−DNA interaction, but when the data are plotted with the other solutes, as shown

Table 1: Values of Δn_w for DNA Melting

cosolute	*E. coli* duplex	AT duplex	TAT triplex
ethylene glycol	3.7	3.6	0.8
glycerol	3.6	2.9	1.1
acetamide	4.4	4.9	2.5
sucrose	7.9	8.1	1.8
average	3.9[a] ± 0.4	3.8[a] ± 0.9	1.2[b] ± 0.5
global fit	4.3 ± 0.5	3.6 ± 0.7	0.9 ± 0.4

[a] The average does not include the value for sucrose. [b] The average does not include the value for acetamide.

in Figure 4, the sucrose points fall within the 95% confidence limits of the full data set. A divergence is also seen for the triplex melt, with acetamide showing a slope significantly different from the rest. If one averages the triplex data with the data for all four sets, the average value of Δn_w is 1.5 ± 0.8, while if the acetamide data are excluded, the average is 1.2 ± 0.5. Thus, the influence of this one set on the overall average is relatively minimal.

The global fit yields values of 3.9 waters per base pair released on melting of duplex DNA to two single strands for both *E. coli* and poly(dA)·poly(dT) DNA. For triplex poly(dT)·poly(dA)·poly(dT) DNA melting to a duplex and single strand, there is approximately one water molecule released per base pair. Thus, we conclude that about four water molecules are released per base pair on melting duplex DNA, regardless of whether there is a rather diverse base composition, as with *E. coli* DNA, or whether the sequence is specifically an A strand coupled with a T strand. For the unravelling of a single strand from the triplex, one water per base triplet is released.

Release of Sodium Ions upon Melting. Sodium ions are known to be bound to DNA in its various forms, these condensed ions contributing to the stability of the helical structures by reducing the repulsive forces between phosphate groups along the chain (*3*, *4*). When the B-form of DNA melts, there is release of Na^+ ion due to the reduction of charge density along the chain in conversion of duplex, helical DNA to single strands. Thus, in addition to the release of water, changes in the number of associated sodium ions are expected upon melting of the duplex or triplex strands studied here. To determine the effects of condensed ions on the melting behavior, data are required in which the sodium ion activity is changed at constant water activity. Thus, we have measured T_m for the melting of triplex, poly(dT)·poly(dA)·poly(dT), and duplex, poly(dA)·poly(dT), in various concentrations of ethylene glycol, containing three different concentrations of NaCl. From these data sets, one can obtain the variation of T_m with salt concentration at several different fixed values of water activity. Figure 6 shows the data for experiments on melting of duplex poly(dA)·poly(dT) in NaCl concentrations of 0.14, 0.21, and 0.29 M, in ethylene glycol solutions with different water activities (determined from osmotic pressure measurements). Similar results were obtained for the triplex melts. Fitting these data by linear regression allows calculation of T_m in pure water or at other water activities for the three salt concentrations.

From eq 3, at a constant water activity and cosolute concentrations, the equilibrium constant for melting of DNA should depend on the salt content of the medium. This leads to the following relationship when converted into the melting temperature, the slope of a plot of T_m^{-1} versus ln $C_\pm$ being

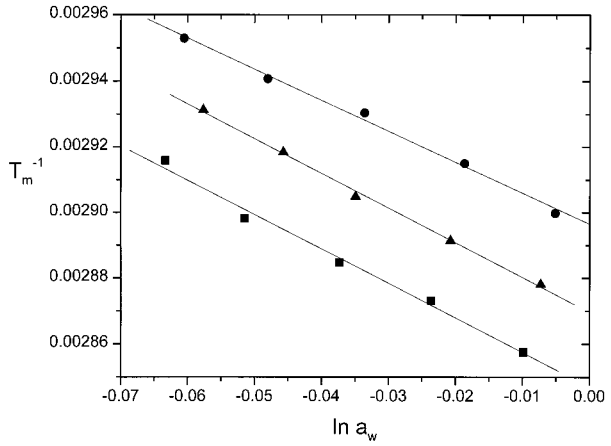

FIGURE 6: Variation of the reciprocal melting temperature of duplex poly(dA)·poly(dT) with the logarithm of water activity in ethylene glycol solutions containing 0.14 (●), 0.21 (▲), and 0.29 M NaCl (■).

Table 2: Values of Δn_{Na^+} per Phosphate for Duplex and Triplex DNA

	AT duplex		TAT triplex	
ln a_w	slope[c] ($\times 10^5$)	Δn_{Na^+}	slope ($\times 10^4$)	Δn_{Na^+}
0.00[a]	−6.05	0.10	−2.92	0.16
0.00[b]	−7.19	0.12	−3.64	0.23
−0.02	−6.89	0.12	−3.44	0.22
−0.04	−6.44	0.11	−3.23	0.20

[a] The values in this row are obtained in the salt solutions between 0.14 and 0.29 M NaCl, so the activity of water is not truly 1. [b] Values in this row are obtained from extrapolation to a water activity of 1 from the ethylene glycol solutions. [c] The slopes are for the T_m^{-1} vs ln $C_\pm$ plots. $\Delta H°$ values of 6870 cal/mol of base pairs for duplex and 3360 cal/mol of triple pairs from Haq (*46*) were used. Errors in the regression coefficients for the slopes average about 5%.

related to Δn_{Na^+}, the change in the number of moles of Na^+ ion bound on melting of the DNA chains:

$$-\frac{\Delta H°}{R}\left[\frac{d(T_m^{-1})}{d(\ln C_\pm)}\right] = \alpha \Delta n_{Na^+} \qquad (7)$$

$\Delta H°$ is the enthalpy of melting per nucleotide (phosphate), and the factor α accounts for the variation of the activity coefficients of the ions with salt concentration, and conversion of ionic activities to concentration, and has a value of about 0.9 in this range of salt concentrations. Record et al. (*4*) have pointed out that eq 7 does not take into account the nonideality of the DNA polyelectrolyte, and they present arguments which suggest that the actual change in sodium ion fraction may be a factor of 2 larger if nonideal screening interactions are accounted for. We will use eq 7 directly, and report in Table 2 the slopes of plots of T_m^{-1} versus ln $C_\pm$ and the values of the number of sodium ions released per phosphate, Δn_{Na^+}, upon melting. The range of values for Δn_{Na^+} is dependent on the measured calorimetric $\Delta H°$ per nucleotide for duplex and triplex melts. As mentioned above, we choose the values of Haq (*46*) because the DNA sources are similar to ours.

Figure 7 shows plots for T_m^{-1} in pure water for the duplex and triplex forms of DNA at the three different salt concentrations. Values shown for pure water in Table 2 and in Figure 7 are obtained from extrapolation to pure water

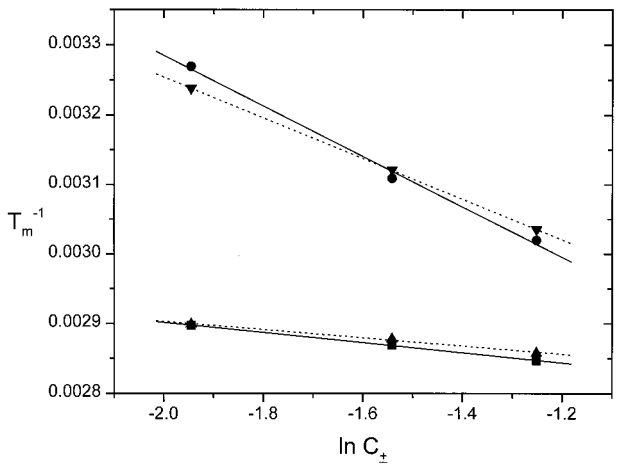

FIGURE 7: Variation of the reciprocal melting temperature for triplex poly(dT)·poly(dA)·poly(dT) (upper curves) and duplex poly(dA)·poly(dT) (lower curves) with the logarithm of salt concentration for solutions with a water activity of 1 (solid lines and points) and with a water activity corresponding to the individual salt solutions (dashed line).

from the ethylene glycol solutions. Other water activities are also shown in Table 2 that are calculated from the regression equations from Figure 6. The data in Table 2 indicate that there is a slight dependence of Δn_{Na^+} on water activity. The values for triplex vary from 0.23 to 0.20 as the water activity changes from 1 to 0.96. For duplex, the change is even smaller, and within the experimental error is invariant over the same variation of water activity. Also shown in Figure 7 and Table 2 are values based on the slopes in the salt solutions in water, but not extrapolated to pure water. In most of the studies of ion binding, the measurements are taken in solutions of NaCl in a specific range of concentrations, typically from a few hundred millimolar to tenths of millimolar. These solutions do have osmotic contributions that will affect T_m slightly, and thus, the slopes of plots of T_m^{-1} versus ln $C_\pm$ will be different from those obtained through extrapolation to water activities of 1. For example, in the poly(dT)·poly(dA)·poly(dT) system if one uses the slopes obtained from plots of the salt solutions containing no ethylene glycol, that is, just NaCl ranging from 0.14 to 0.29 M, then the value of Δn_{Na^+} comes out to be 0.16 rather than 0.23 for the triplex melt. For duplex, the value is 0.10 versus 0.12. Ion release on melting of the triple helix is thus dependent not only on what the salt content is, but also somewhat on the water activity of the medium. Most of previous melting studies have been carried out in NaCl solutions in buffer, and thus, values of Δn_{Na^+} contain a slightly perturbing effect of the osmotic contribution of the salt.

The ion release numbers (Δn_{Na^+}) are in reasonable agreement with the data of Krakauer and Sturtevant (*47*). Triple-helical poly(U)·poly(A)·poly(U) gives a change of 0.10 sodium ion per phosphate, relative to 0.16 ion for poly(dT)·poly(dA)·poly(dT) found here. The number 0.16 is used since the values of Krakauer and Sturtevant are not based on extrapolation to a water activity of 1. Their result for melting of poly(A)·poly(U) is a release of 0.16 Na^+ ion per phosphate, compared with 0.10 determined here for poly(dA)·poly(dT). The results are also in reasonable agreement with values obtained by Zieba et al. (*48*) for small decamers (0.14). The consequences of these sodium ion releases will be considered later.

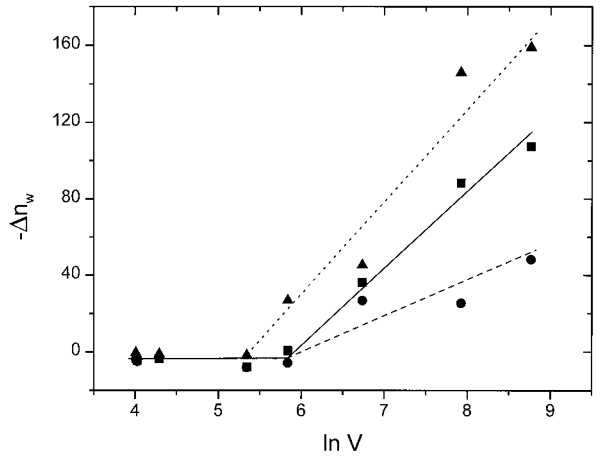

FIGURE 8: Change in the number of waters released upon melting of DNA for *E. coli* duplex (■ and solid line), poly(dA)·poly(dT) duplex (● and dashed line), and triplex poly(dT)·poly(dA)·poly(dT) (▲ and dotted line) with a molar volume of cosolute. Positive values of $-\Delta n_w$ correspond to water release. The solutes used [and molar volume (milliliters per mole) in parentheses] were acetamide (56), ethylene glycol (55), glycerol (73), sucrose (215), PEG 400 (343), PEG 1000 (845), PEG 3400 (2770), and PEG 8000 (6650).

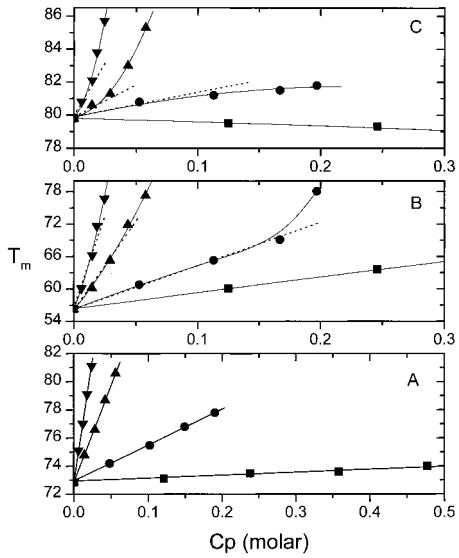

FIGURE 9: Variation of the melting temperature of DNA with the molar concentration of the polyethylene glycol cosolute for (A) *E. coli* duplex, (B) poly(dT)·poly(dA)·poly(dT) triplex, and (C) poly(dA)·poly(dT) duplex. Cosolutes were (■) PEG 400, (●) PEG 1000, (▲) PEG 3400, and (▼) PEG 8000. The dashed lines are the limiting slopes used in the calculation of the excluded volume.

Effects of Higher-Molecular Weight Cosolutes. To study the influence on thermal melting of DNA of higher-molecular weight cosolutes, a series of solutions containing PEGs with increasing molecular weights were tested with the duplex and triplex DNA. An illustration of the effect of these larger volume solutes on the melting of triplex and duplex DNA is shown in Figure 8, in which Δn_w, calculated from eq 6, is plotted as a function of the molar volume of the cosolute. The low-molecular weight osmolytes are included, and indicate that when the molar volumes reach somewhere between 200 and 300 mL/mol, there is a major change in the behavior of Δn_w, with the larger solutes producing very large and opposite effects compared with the smaller cosolutes. Since the effect of the smaller solutes is virtually constant, it is logical that these perturbants are producing their effects through changes in water activity, as analyzed above. For the larger solutes, the changes depend on molar volume; thus, it is likely that these effects are due to volume exclusion by the solutes and DNA, producing increases in melting temperature rather than decreases with increasing concentrations of solute. Woolley and Wills (*35*) have analyzed the increased T_m of RNA [poly(I)·poly(C)] in the presence of high-molecular weight polymers of PEG or dextran in terms of volume exclusion. Their approach is to treat volume exclusion as an effect on the activity coefficients of the DNA components, e.g., the duplex and single strands, and thus during the melting process, the changes in excluded volume with increased cosolute concentration directly affect the melting temperature. The equation for T_m in the presence of higher-molecular weight polymers is

$$T_m = T_m^\circ + \frac{RT_m^{\circ 2}}{\Delta H}(\Delta V_{ex})C_p \qquad (8)$$

where C_p is the molar concentration of polymer, ΔV_{ex} is the change in excluded volume upon melting, T_m° is the melting temperature in the absence of polymer, and ΔH is the enthalpy of melting of the DNA. Thus, plots of T_m versus C_p should be a straight line, the slope of which allows calculation of the excluded volume change, ΔV_{ex}.

Because these cosolutes also affect the melting temperature in the opposite direction through changes in water activity, it is necessary to correct the values of T_m for the osmotic pressure effect (*39*). Although these corrections are small, particularly for the higher-moleculer weight polymers, the plots shown in Figure 9 were corrected for the osmotic effect as follows. First, it was assumed that ethylene glycol would exhibit its effect as purely a water activity influence. Plots of T_m versus osmolality for ethylene glycol were prepared, which were linear, and a regression equation was obtained for each DNA case studied. Then, from the measured osmolality of the copolymers, a correction was calculated on the basis of the ethylene glycol data, and this correction was then added to the T_m value for each of the polymer solutions. In most cases, this correction was $<1°$, since the osmolalities of the polymers are small relative to that of ethylene glycol at an equivalent weight percent. The data plotted in Figure 9 show the corrected T_m values as a function of molar concentration.

The plots in Figure 9 for *E. coli* and the triplex show expected behavior; that is, with increasing copolymer molecular weights, there is an increased slope, and thus a larger excluded volume, and all cosolutes show positive slopes. For duplex, poly(dA)·poly(dT), however, there are clear inconsistencies with the other data sets. First, the slope for PEG 400 has a negative value, indicating a change in excluded volume that is opposite of the others. One would expect the values of ΔV_{ex} for poly(dA)·poly(dT) melting to be similar to those for *E. coli*, since they are both changing from duplex to two single strands. The excluded volumes for the duplexes and melted single strands ought to be similar in size. Table 3 shows the calculated values for the duplex and triplex samples studied. The changes in excluded volume for poly(dA)·poly(dT) are somewhat smaller than those for *E. coli*, particularly for the larger polymers. This factor suggests that the two DNA samples are behaving differently with regard

Table 3: Excluded Volume Changes (ΔV_{ex}) for DNA Copolymer Components[a]

copolymer	TAT triplex[b]	AT duplex	*E. coli* duplex	V_{ex}(dup)[c]	V_{ex}(dup)[d]
PEG 400	0.45	−0.025	0.079	0.92	0.82
PEG 1000	1.33	0.47	0.85	2.20	1.80
PEG 3400	5.10	1.45	4.56	8.75	5.64
PEG 8000	11.80	4.30	11.28	19.70	12.80

[a] Values are in liters per mole. [b] These are also equal to V_{ex}(ss). [c] Excluded volume of the duplex copolymer based on the AT duplex ΔV_{ex}. [d] Excluded volume for the duplex copolymer based on *E. coli* ΔV_{ex}.

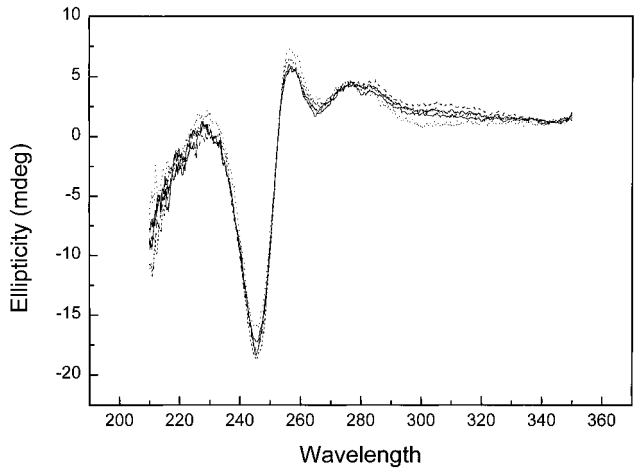

FIGURE 10: Circular dichroism spectra of triplex poly(dT)·poly(dA)·poly(dT) in 20% ethylene glycol (solid line), 15% PEG 400 (dotted line), 5% PEG 3400 (dashed line), 5% PEG 8000 (short dashed line), and CNE buffer (solid line).

to excluded volume, suggesting a different conformational organization in the two cases. For this reason, we examined CD spectra for the majority of the solutions studied.

There are a number of studies published that suggest that at high concentrations of copolymers and with a high salt content in the DNA solutions condensed phases appear (*49*, *50*). In solutions of ethanol (30−50%) containing reasonably high salt concentrations (0.2−0.5 M), these condensed forms, designated $\psi(+)$ or $\psi(-)$, depending on the effect on the CD spectrum, are characterized as cholesteric liquid crystalline phases, and suggest long-range ordering in solutions of this type (*49*). Chaires (*50*) reported similar effects of polyethylene glycol on the physical state of poly(dA)·poly(dT), solutions of 15% (w/v) PEG 8000 showing evidence of the $\psi(+)$ phase. These long-range aggregation reactions are accompanied by anomalously large positive changes in the CD spectra. Thus, it was important to examine CD spectra for the solutions used in these studies. For the *E. coli* samples in BPE buffer (16 mM Na^+), there was no evidence of change in the CD spectrum from B-form DNA, even at the highest (20% PEG 8000) concentrations. The CD spectra in ethylene glycol or any of the other copolymers showed virtually no difference from the spectrum in buffer alone. However, for the triplex, poly(dT)·poly(dA)·poly(dT), there were some changes in the CD spectra, depending on concentration and which copolymer was present in the buffer (CNE with 0.3 M NaCl). Figure 10 shows the superposition of several spectra of the triplex in different media. In all of these solutions, the CD spectra are similar to those for the triplex in buffer alone. There are only minor changes in the

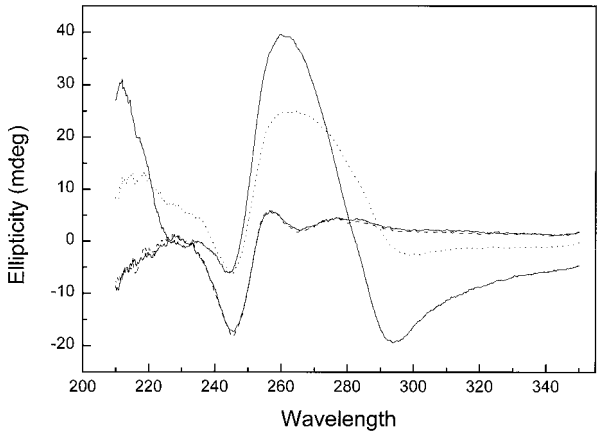

FIGURE 11: Circular dichroism spectra for solutions of triplex poly(dT)·poly(dA)·poly(dT) in solutions of 10% (dashed line), 15% (solid line), and 20% (dotted line) PEG 1000. The solid line superimposed on the 10% PEG line is the spectrum in CNE buffer alone.

intensities of the bands at 246 and 253 nm. Thus, there appear to be no major conformational changes in these solutions. At higher concentrations of the larger copolymers (PEG 1000, PEG 3400, and PEG 8000), significant changes in the CD spectra are observed. Figure 11 shows the spectra of the triplex in buffer and in 10−20% (w/v) PEG 1000. The 10% solution spectrum closely resembles the spectrum in buffer. However, increasing to 15 and 20% produces large changes in the CD bands. The spectrum in 20% PEG 1000 is quite similar to the $\psi(+)$ spectra reported by Huey and Mohr (*49*) and by Chaires (*50*) for duplex poly(dA)·poly(dT). The $\psi(+)$ state is thought to be a supramolecular aggregate of twisted DNA strands, leading to chirality which can be either positive or negative depending on the handedness of the twist (*49*). In the DNA cases studied here, we expect that some of the solutions have these aggregated forms present. Solutions of triplex, poly(dT)·poly(dA)·poly(dT), or duplex, poly(dA)·poly(dT), in which the concentration of PEG 1000 or PEG 3400 is greater than 10% show evidence of the supramolecular structures. For PEG 8000, even the 10% solutions have positively enhanced CD spectra.

The consequences of these higher-order aggregations to the melting of DNA are not totally clear. Huey and Mohr (*49*), as well as Gray et al. (*51*), argue that despite the aggregation to ψ-DNA, there is virtually no change in the secondary structure of the DNA chains. That is, within the aggregates the normal B-form DNA persists. If this were true, then one expects that melting transitions would be affected through changes in excluded volume due to the aggregated structures. For the melting of duplex DNA, aggregation of the duplex to polymorphic phases would lead to an increased excluded volume for the duplex relative to single strand, and thus according to eq 7 would lead to lowered ΔV_{ex} values compared with the case in the absence of any aggregation. For triplex aggregation, the effect on T_m would depend on the relative extent of aggregation of the triplex relative to duplex, since the expected change is

$$\Delta V_{ex} = V_{ex}(\text{ss}) + V_{ex}(\text{dup}) - V_{ex}(\text{tri}) \qquad (9)$$

If there is a higher degree of aggregation for the duplex, positive increases in ΔV_{ex} would be expected, while more

aggregation in the triplex form would lead to smaller slopes. In Figure 9, it is clear that for the larger copolymers there is a positive deviation from a linear response for the triplex melts, particularly at higher concentrations. This is consistent with the duplex being more extensively aggregated than the triplex. Note also in Figure 9 that the curves for *E. coli* are perfectly linear, showing no effects of aggregation. The duplex poly(dA)·poly(dT) melting transitions are somewhat difficult to understand. As mentioned above, that for the PEG 400 actually shows a negative slope; that for PEG 1000 shows a positive increase, and there is a negative deviation from linearity for this copolymer, as might be expected for association of the duplex. However, the examples with higher-molecular weight copolymers, PEG 3400 and 8000, both show positive deviations from linearity. The curvature in the T_m versus C_p plots complicates the evaluation of ΔV_{ex} somewhat. However, if it can be assumed that as the concentration of copolymer approaches zero, these higher-order aggregates will disappear, as the CD spectra indicate, then one could use the limiting slopes of the T_m versus C_p plots to evaluate ΔV_{ex}. For the triplex and duplex, poly(dA)·poly(dT), the values of ΔV_{ex} shown in Table 3 are calculated from the limiting slopes, while for *E. coli*, linear regression was used to obtain the change in excluded volumes.

To explore further the excluded volume effects in the PEG solutions studied, an additional calculation can be made that is useful. According to eq 8, the change in excluded volume for the triplex melting transition is related to the difference between the sum of the volumes for single strand and duplex and the volume for the triplex. Because the effective radii of duplex and triplex polynucleotides are similar in magnitude, e.g., 1.18 nm for duplex and 1.21 for triple-helical poly(A)·poly(U)·poly(A) (*52*), the excluded volumes of duplex and triplex with a copolymer such as PEG ought to be similar. Thus, from eq 8 to a first approximation, the measured ΔV_{ex} of the triplex should be close to the actual excluded volume of the single-strand poly(dT) with copolymer. That is, $\Delta V_{ex}(\text{tri}) = V_{ex}(\text{ss})$. If we assume that this is true, then it is possible to calculate the actual excluded volumes for duplex *E. coli* and for duplex poly(dA)·poly(dT) from the experimental excluded volume changes for the duplex, and the value of V_{ex}(ss) obtained from the triplex data. For *E. coli*, $\Delta V_{ex}(E.coli) = 2V_{ex}(\text{ss}) - V_{ex}(\text{dup})$, and a similar expression applies for the duplex poly(dA)·poly(dT). The values of V_{ex} for the single strand and duplex are included in Table 3. In principle, the values of V_{ex}(dup) for the two types of DNA ought to be equal, but there is significant divergence for the larger PEGs. Because of the peculiarities of the poly(dA)·poly(dT) T_m versus C_p curves in Figure 9, it is not unexpected that this case might be different. The magnitude of V_{ex}(dup) based on the calculation from the *E. coli* ΔV_{ex} is thus more reliable than that based on the poly(dA)·poly(dT) value and, as will be seen below, is also in good agreement with a calculated excluded volume for duplex based on simple geometric models.

DISCUSSION

Hydration of DNA. The various methods used to estimate DNA hydration yield results that depend on what properties are being probed. Measurements of the water of hydration by densitometry or ultrasonic measurements and calorimetry generate numbers in the range of 15−20 water molecules per base pair (*18*, *20*). A number of studies indicate that water may exist in several different states when associated with the hydration shells of DNA (*18*−*20*). Thus, some of the 15−20 water molecules per base pair may be quite labile and, although associated with the DNA, rapidly exchange with bulk water (*15*, *53*). Infrared and NMR measurements on DNA solutions have led to suggestions that there are water molecules that specifically interact with the phosphates and ribose rings of the DNA backbone in both duplex and single-stranded forms (*12*, *13*). In addition, hydration within the base pairing region has been postulated to explain a variety of experimental studies of the stability of various forms of DNA (*7*, *8*). These studies address the apparent presence of water in the major and minor grooves of duplex DNA, and its role in the stability and transformation between secondary structural forms.

Perhaps the most effort in trying to understand associated water in DNA has been expended in analyzing the crystal structures of oligomeric DNA (*7*−*9*). These studies have led to a variety of postulates regarding the presence and role of groove-bound water. From the early paper by Drew and Dickerson (*54*), which suggested that AATT tracts in a dodecamer show evidence of a spine of hydration in the minor groove and ribbons of water in the wider sections, a number of papers have appeared with analysis of a variety of crystals, ranging from hexamers to 20-mers. In all of these analyses, the water is found bound in locales that show specific hydrogen bonding interactions with bases, and in some cases with the ribose oxygens and phosphates (*9*). The rate of exchange of these waters as measured by NMR spectroscopy is much slower than those of other hydration water, particularly for those molecules of water thought to be associated with the minor groove of A_nT_n tracts (*55*−*57*). A recent paper by Shui et al. (*58*), on the X-ray structure of a dodecamer similar to the Drew−Dickerson dodecamer, under very high resolution shows that the spine of hydration in the AT tract is two layers deep, and is partially occupied by sodium ions. Thus, there seems to be clear evidence for uniquely bound water in a variety of DNA structures. The question then arises as to what waters we are examining in the osmotic stress measurements.

In the osmotic stressing measurements on the melting of duplex to single strands, the values of Δn_w represent the difference in uniquely bound waters to the duplex relative to single strands. As pointed out by Parsegian et al. (*21*), water that is osmotically significant has its chemical potential altered by the presence of the macromolecule and thus is different from the bulk solvent. In addition, in the case of melting experiments, it is possible that water that may be different from bulk water is the same in both single strand and duplex. This may be true for more labile waters associated with the surface phosphates or ribose sites, since these sites are available to water in both duplex and single strand. Thus, the changes in hydration associated with the melting transition represent waters that are uniquely bound to the duplex and released to bulk water in the single-strand state. Our data suggest that about four water molecules per base pair are released when the DNA duplex melts, and that it does not depend on the sequence, since poly(dA)·poly(dT) and *E. coli* duplexes both give up about four waters. Schneider and Berman (*17*) have analyzed crystal structures

of 14 B-DNA decamers and find evidence for about five water molecules hydrogen bonded in the base region. The data show the same extent of hydration of guanine and adenine, and of cytosine and thymine. If it is assumed that these water molecules are released from the duplex upon melting, and that single strands do not bind any of the liberated waters, the data would be approximately consistent with our hydration changes.

The new X-ray data of Shui et al. (*58*) show a model for B-DNA that includes both sodium ions and water molecules sharing sites in the spine of hydration with a secondary layer of water on top of the primary spine. These complexes could easily result in four or five molecules of water per base pair being uniquely bound in the duplex. We thus conclude that the values of Δn_w are reasonably consistent with the release of water bound within the duplex that have been suggested from X-ray analysis.

It is striking that our results show no difference in Δn_w for a natural DNA (*E. coli*) and poly(dA)·poly(dT) duplex. Poly(dA)·poly(dT) normally shows evidence of a spine of hydration in its melting behavior (*44*). There is a broad premelting transition (midpoint at 29.9 °C) thought to be due to the disruption of the bound water in the spine of hydration in the minor groove of the duplex. In our case, the poly(dA)·poly(dT) in solution is derived from the melting of the triplex poly(dT)·poly(dA)·poly(dT), with the single strand unravelling at temperatures near 56 °C. At this temperature, the spine of hydration in the minor groove of poly(dA)·poly(dT) would be largely disrupted. Herrera and Chaires (*44*) suggest on the basis of changes in CD spectra, changes in the susceptibility to DNase I digestion, and characteristic changes in drug binding that disruption of this minor groove water results in a conformational change in poly(dA)·poly(dT), a change that makes the duplex a more normal B-form. Thus, this more "normal" B-form poly(dA)·poly(dT) may be hydrated in a manner similar to that of the *E. coli* duplex conformation, and water release upon melting is virtually the same for both.

The release of only one water molecule when triplex poly(dA)·poly(dT)·poly(dA) melts to single strand and duplex suggests a small number of uniquely bound waters in the triple helical structure. Several studies support this result. Using NMR relaxation methods, Radhakrishnan and Patel (*14*) provide evidence that there are water molecules bound in the new Watson−Hoogstein or Crick−Hoogstein grooves formed in triple-helical structures. A molecular dynamics simulation also shows a spine of hydration in triple-helical grooves, and the simulations show a persistent single water molecule per triple base within the groove (*59*). So, again if this water molecule is released upon melting of the third strand to form duplex and single strand, our value of Δn_w for triplex melting is consistent with the hydrated triplex structures proposed from X-ray analysis.

In summary, it should be emphasized that duplex and triplex DNA are more highly hydrated than is indicated from the osmotic stressing experiments reported here. That is, there are many more water molecules along the surfaces of the DNA that would be significant, for example, in drug or protein binding to the DNA surface. In the strand separation of melting, however, the water molecules that are significant are those which are tightly bound within the duplex or triplex, and are the ones mostly likely important in playing a role in the conformation and stability of the DNA structures. Thus, any solution condition that can alter water activity will undoubtedly have an effect on the stability of a particular conformation through influence on these bound water molecules. Changes in the osmotic environment within the cell then could alter the conformation of DNA through subtle changes in the displacement of water from the structure.

Ion Release upon Melting. Experimental evidence for ion release upon the melting of DNA has been well-established. These data are usually analyzed using the Manning model or variations of that model proposed by Record (*3*−*5*). The key idea of these models is that there is condensation of ions along the surface of the DNA due to the relatively high charge density along the chain. The charge density parameter (ξ) is related to the axial charge separation along the DNA chain (b) by the equation $\xi^{-1} = b/7.14$, the factor of 7.14 being the Bjerrum length (angstroms) from the Manning model (*3*). Values of b have been estimated from X-ray data to be about 1.7 Å in duplex form, since there are two phosphates per 3.4 Å along the helix axis, and since the fraction of counterion bound per phosphate is $1 - \xi^{-1}$, these numbers predict that the fraction of sodium bound per phosphate is 0.75 for typical B-form DNA. From experimental measurements of sodium ion release upon melting, one can determine Δn_{Na^+} as described above. Record et al. (*4*) have suggested that the true stoichiometric amount of sodium release is strongly affected by nonideal interactions between the polyelectrolyte DNA and sodium ions. Thus, the use of eq 7 above leads to Δn_{Na^+} values that are too small by a factor of 2. Accordingly, the values for sodium ion release shown in Table 2 could be underestimated. In the analysis of Record, he multiplies the experimental Δn_{Na^+}, obtained from plots of T_m^{-1} versus ln C_{Na^+}, by 2 to determine the release of Na^+ upon melting of duplex to single-stranded DNA. Since $\Delta n_{Na^+} = \xi^{-1}(ss) - \xi^{-1}(dup)$, it is possible to determine the fraction of ions bound to single strand (*3*, *4*). For typical natural DNA, Δn_{Na^+} values from slopes of the inverse temperature versus ln C plots are about 0.185, so the stoichiometric release is about 0.37 ion per phosphate. Using that figure for ion release leads to 0.38 counterion per phosphate in single-stranded DNA.

Poly(dA)·poly(dT) duplex DNA is not a typical B-form structure (*60*−*62*); however, the value of b is not too different from that for natural DNA, 1.5 vs 1.7 Å (*60*). This leads the fractional binding of counterions to increase slightly to 0.78. Using our value for Δn_{Na^+} of 0.25 (2×0.12) leads to an average of 0.53 sodium per phosphate for the single strands, poly(dA) and poly(dT). Polyadenylic acid, poly(A), was found to have a somewhat smaller value of b than poly(U), 3.1 vs 4.5 Å, respectively (*4*). Thus, the fractional occupancy of phosphate sites by sodium for single-stranded poly(A) is 0.56, while the occupancy is more like that for natural DNA single strands (0.36) for poly(U). Note that the average is 0.46, not too different from our value of 0.53, and suggests the possibility that the value for poly(dA) may also be somewhat higher than that for poly(dT). The origin of the differences between A and U or T single strands is thought to arise from the stacking of the adenine bases in the single strand, thus shortening the distances between phosphates (*2*). However, our understanding of the conformation of single-stranded DNA in solution, and thus the phosphate spacing,

is limited, and thus, the results we report here for single strand ion condensation can only be approximate.

The transition from triplex with a very high charge density along the helix, and thus a large number of condensed sodium ions, to duplex and single strand ought to release significant numbers of ions. Our data indicate that 0.46 (2 × 0.23) ion per phosphate site are released in the melting process in pure water or 0.32 (2 × 0.16) ion if measured in salt solution (see Table 2). One can estimate the level of ion release on the basis of the data presented by Record et al. (*4*) for poly(U)·poly(A)·poly(U) triplex. Their value for the extent of sodium ion binding is about 0.85 for triplex and 0.75 for duplex. The problem in our case is what to use for single-stranded poly(dT). If the single strand value of 0.38 for natural DNA is used, then one can calculate the extent of ion release on melting of triplex to duplex and single strand.

$$\Delta n_{Na^+} = 0.85 - {}^2/_3 \times 0.75 - {}^1/_3 \times 0.38 = 0.23$$

Since most ion binding studies are carried out in salt solutions without extrapolation to pure water, our value of 0.33 would be more comparable to the above calculation. Although somewhat higher, the agreement is most likely within the possible errors. The assumptions about values for specific ion binding to the various forms of DNA could be in error. Differences of a few hundreths in the parameters used can affect the calculation significantly. An additional factor that should be mentioned is that the values of Δn_{Na^+} are directly dependent on the values of calorimetric $\Delta H°$ used in the calculation. Errors of 10% could lead to corresponding errors in the extent of ion release so that values used for calculation of ion binding may have systematic errors related to the choice of enthalpy of melting. In any case, it seems clear that triplex DNA will have a high degree of counterion association (0.85−0.90), while the values for duplex and single strand are substantially lower (0.75 for duplex and 0.35−0.60 for single strand, depending on the base composition). The binding is clearly dependent upon the charge density along the chain, but also is dependent upon the osmotic status and concentrations of ions in the surrounding medium, as the data in Table 2 indicate. Thus, in the evaluation of counterion association with DNA, it is important to map out both the ionic concentration effects and the associated status of water activity in the medium.

Excluded Volume Effects. The measured excluded volumes presented above in Table 3 can be used to examine models for the excluded volume effect. Several authors have used simple geometric models to estimate the excluded volumes for crowded solutions (*35*−*38*). A reasonable model for DNA−PEG exclusion would be a DNA cylinder in contact with a spherical copolymer of PEG. If end effects are neglected, the volume excluded by such geometry is a cylinder around the circumference of the DNA whose radius is the sum of the radius of DNA and the effective radius of the copolymer. The excluded volume can be calculated from the simple equation

$$V_{ex} = \Pi N_A L (R_{DNA} + R_{Pol})^2 \qquad (10)$$

where N_A is Avogadro's number so that the volume can be calculated on a molar basis and L is the length of the cylindrical segment, in this case the distance between base pairs or triplet, because in calculating the experimental ΔV_{ex}, the numbers were per base pair (triplet). R_{DNA} is the radius of the appropriate DNA component, and R_{Pol} is the radius of the copolymer. Since the radii of single-stranded, duplex, and triplex DNA are known, the problem is to define an effective radius for the copolymer. An approach for the data obtained here is to again rely on the measured excluded volume of the triplex as V_{ex}(ss), and then use the radius of single-stranded DNA in eq 9 to allow calculation of R_{Pol}. Table 4 shows the values of the PEG radii determined this way, and shows that the values are somewhat larger than the hydrodynamic radii of the PEGs (*63*). With these estimates of R_{Pol}, it is now possible to calculate V_{ex}(dup), the excluded volume for duplex DNA with the PEG copolymers. These numbers are shown in Table 4. Also, Figure 12 shows comparisons with the measured values of V_{ex}(dup) for the *E. coli* and poly(dA)·poly(dT) duplexes. The calculated V_{ex}(dup) values are reasonably close to the experimental values, but are somewhat larger than the *E. coli* numbers, which should be the most reliable, and smaller than the experimental values for poly(dA)·poly(dT). The calculated excluded volumes are quite sensitive to the values of R_{Pol}. Decreasing R_{Pol} by a few tenths of a nanometer improves the agreement with the experimental values for *E. coli*, as shown in Figure 12, where a recalculated set of values for V_{ex}(dup) are presented on the basis of slightly smaller R_{Pol} numbers. The recalculated numbers are in excellent agreement with the *E. coli* data in Table 3, and the values of R_{Pol}, although larger than hydrodynamic radii, are not unreasonable for the PEG polymers. These calculations add

Table 4: Calculated Radii and Excluded Volumes for DNA Duplexes with Copolymer[a]

copolymer	R(hyd)[b]	R_{Pol}(calc)	V_{ex}(du)[c]	R_{Pol}(adj)	V_{ex}(du)[d]
PEG 400	0.67	0.30	1.20	0.15	1.00
PEG 1000	0.87	0.90	2.50	0.60	1.86
PEG 3400	1.60	2.26	7.30	1.90	5.80
PEG 8000	2.70	3.77	15.20	3.40	13.00

[a] Radii are in nanometers. Volumes are in liters per mole. [b] Hydrodynamic radii from Kuga (*63*). [c] Calculated excluded volume of the duplex using R_{Pol} from column 3. [d] Calculated excluded volume of the duplex using R_{Pol} from column 5.

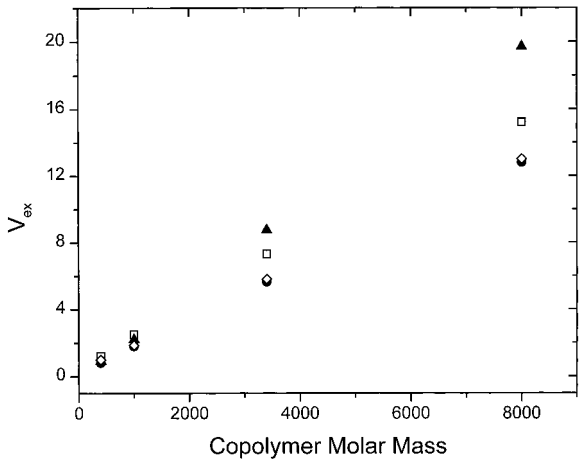

FIGURE 12: Experimental excluded volumes for (▲) poly(dA)·poly(dT) and (●) *E. coli* DNA plotted vs the molar mass of the copolymer. Also included are the calculated excluded volumes using eq 9 and (□) R_{Pol} values from column 3 of Table 4 and (◇) using R_{Pol} values from column 5 of Table 4.

support to the conclusion that the effect on T_m for the larger cosolutes is basically an excluded volume effect that can be successfully modeled as cylinder-sphere geometry. The fact that the poly(dA)·poly(dT) volumes do not agree with the calculated values as well as with the *E. coli* volume could be a result of the peculiarities of the measured values for poly(dA)·poly(dT), as mentioned above.

CONCLUSIONS

The data and analysis presented in this paper confirm that in addition to fundamental interactions between base pairs and phosphate charges, conditions in solution play an important role in the stability of DNA duplex and triplex structures. Because DNA secondary structure is influenced by the presence of water molecules within the duplex and triplex chains, any changes in the osmotic environment of the cell can influence the number of water molecules associated, and thus could determine the stability or conformation of the helical structures. Clearly, the stability of triplex and duplex DNA is also influenced by the availability of space within its environment. A crowded environment produces a marked stabilizing effect on triplex structures, and to a lesser extent on duplex DNA. Since the cell contains a vast array of macromolecules that can exclude volume, it is likely that the physical and chemical behavior of DNA within those crowded spaces will be affected. Finally, the known role of sodium ion in influencing the stability of duplex and triplex DNA is confirmed. The combination of these environmental conditions clearly plays a major role in the thermodynamic properties of DNA in the cell.

ACKNOWLEDGMENT

We thank Ihtshamul Haq of the University of Greenwich (Greenwich, U.K.) for providing unpublished calorimetric enthalpies for the melting of triplex poly(dT)·poly(dA)·poly(dT) and duplex poly(dA)·poly(dT). We thank Dr. Xiaogang Qu for osmotic pressure measurements and for reading a draft of the manuscript.

REFERENCES

1. Adams, R. L. P., Knowler, J. T., and Leader, W. P. (1992) *The Biochemistry of Nucleic Acids*, 11th ed., Chapman and Hall, New York.
2. Saenger, W. (1984) *Principles of Nucleic Acid Structure*, Springer-Verlag, New York.
3. Manning, G. S. (1972) *Biopolymers 11*, 937−949.
4. Record, M. T., Anderson, C. F., and Lohman, T. M. (1978) *Q. Rev. Biophys. 11*, 103−178.
5. Anderson, C. F., and Record, M. T. (1990) *Annu. Rev. Biophys. Biomol. Struct. 19*, 423−465.
6. Texter, J. (1978) *Prog. Biophys. Mol. Biol. 33*, 83−97.
7. Berman, H. M. (1991) *Curr. Opin. Struct. Biol. 1*, 423−427.
8. Berman, H. M. (1994) *Curr. Opin. Struct. Biol. 4*, 345−350.
9. Kochoyan, M., and Leroy, J. L. (1995) *Curr. Opin. Struct. Biol. 5*, 329−333.
10. Westhoff, E. (1988) *Annu. Rev. Biophys. Biophys. Chem. 17*, 125−144.
11. Falk, M. (1966) *Can. J. Chem. 44*, 1107−1111.
12. Falk, M., Hartman, K. A., and Lord, R. C. (1963) *J. Am. Chem. Soc. 85*, 391−399.
13. White, A. P., Reeves, K. K., Snyder, E., Farrell, J., Powell, J. W., Mohan, V., and Griffey, R. H. (1996) *Nucleic Acids Res. 24*, 3261−3266.
14. Radhakrishnan, I., and Patel, D. J. (1994) *Biochemistry 33*, 11405−11416.
15. Radhakrishnan, I., and Patel, D. J. (1994) *Structure 2*, 395−405.
16. Conte, M. R., Conn, G. L., Brown, T., and Lane, A. N. (1996) *Nucleic Acids Res. 24*, 3693−3699.
17. Schneider, B., and Berman, H. M. (1995) *Biophys. J. 69*, 2661−2669.
18. Chalikian, T. V., Saravazyan, A. P., Plum, G. E., and Breslauer, K. J. (1994) *Biochemistry 33*, 2394−2401.
19. Rentzeperis, D., Kharakoz, D. P., and Marky, L. A. (1991) *Biochemistry 30*, 6276−6283.
20. Rentzeperis, D., Kupke, D. W., and Marky, L. A. (1993) *Biopolymers 33*, 117−125.
21. Parsegian, V. A., Rand, R. P., and Rau, D. C. (1995) *Methods Enzymol. 259*, 43−94.
22. Sidorova, N. Y., and Rau, D. C. (1996) *Proc. Natl. Acad. Sci. U.S.A. 93*, 12272−12277.
23. Vossen, K. M., Wolz, R., Daugherty, M. A., and Fried, M. G. (1997) *Biochemistry 36*, 11640−11647.
24. Wyman, J. (1964) *Adv. Protein Chem. 19*, 223−286.
25. Wyman, J. (1965) *J. Mol. Biol. 11*, 631−644.
26. Leikin, S., Parsegian, V. A., and Rau, D. C. (1993) *Annu. Rev. Phys. Chem. 44*, 369−395.
27. Arakawa, T., and Timasheff, S. N. (1982) *Biochemistry 21*, 6536−6544.
28. Arakawa, T., and Timasheff, S. N. (1982) *Biochemistry 21*, 6545−6552.
29. Arakawa, T., and Timasheff, S. N. (1985) *Biophys. J. 47*, 411−414.
30. Lee, J. C., and Lee, L. L. Y. (1981) *J. Biol. Chem. 256*, 625−631.
31. Lee, J. C., and Lee, L. L. Y. (1987) *Biochemistry 26*, 7813−7819.
32. Columbo, M. F., Rau, D. C., and Parsegian, V. A. (1992) *Science 256*, 655−659.
33. Reid, C., and Rand, R. P. (1997) *Biophys. J. 72*, 1022−1030.
34. Laurent, T. C., Preston, B. N., and Carlsson, B. (1974) *Eur. J. Biochem. 43*, 231−235.
35. Wooley, P., and Wills, P. R. (1985) *Biophys. Chem. 22*, 89−94.
36. Wills, P. R., and Winzor, D. J. (1993) *Biopolymers 33*, 1627−1629.
37. Winzor, D. J., and Wills, P. R. (1995) *Biophys. Chem. 57*, 103−110.
38. Poon, J., Bailey, M., Winzor, D. J., Davidson, B. E., and Sawyer, W. H. (1997) *Biophys. J. 73*, 3257−3264.
39. Louie, D., and Serwer, P. J. (1994) *J. Mol. Biol. 242*, 547−558.
40. Spink, C. H., and Chaires, J. B. (1995) *J. Am. Chem. Soc. 117*, 12887−12888.
41. Rogers, J. A., and Tam, T. (1977) *Can. J. Pharm. Sci. 12*, 65−70.
42. Wyman, J., and Gill, S. J. (1990) *Binding and Linkage*, University Science Books, Mill Valley, CA.
43. Cohn, E. J., and Edsall, J. T. (1943) *Proteins, Amino Acids and Peptides as Ions and Dipolar Ions*, Reinhold Publishing Co., New York.
44. Herrera, J. E., and Chaires, J. B. (1989) *Biochemistry 28*, 1993−2000.
45. Pilch, D. S., Levenson, C., and Shafer, R. H. (1991) *Biochemistry 30*, 6081−6088.
46. Haq, I. (1996) unpublished results.
47. Krakauer, H., and Sturtevant, J. M. (1968) *Biopolymers 6*, 491−512.
48. Zieba, K., Chu, T. M., Kupke, D. W., and Marky, L. A. (1991) *Biochemistry 30*, 8018−8026.
49. Huey, R., and Mohr, S. C. (1981) *Biopolymers 20*, 2533−2552.
50. Chaires, J. B. (1989) *Biopolymers 28*, 1645−1650.
51. Gray, D. M., Edmondson, S. P., Lang, D., Vaughn, M., and Nave, C. (1979) *Nucleic Acids Res. 6*, 2089−2107.
52. Arnott, S., and Selsing, B. E. (1974) *J. Mol. Biol. 88*, 509−521.

53. Lane, A. N., Jenkins, T. C., and Frenkiel, T. A. (1997) *Biochim. Biophys. Acta 1350*, 205−220.
54. Drew, J. R., and Dickerson, R. E. (1981) *J. Mol. Biol. 151*, 535−556.
55. Kubinec, M. G., and Wemmer, D. E. (1992) *J. Am. Chem. Soc. 114*, 8739−8740.
56. Leipinsh, E., Otting, G., and Wuthricyh, K. (1992) *Nucleic Acids Res. 20*, 6549−6553.
57. Leipinsh, E., Leupin, W., and Otting, G. (1994) *Nucleic Acids Res. 22*, 2249−2254.
58. Shui, X., McFail-Isom, L., Hu, G. G., and Williams, L. D. (1998) *Biochemistry 37*, 8341−8355.
59. Mohan, V., Smith, P. E., and Montgomery, P. B. (1993) *J. Am. Chem. Soc. 115*, 9297−9298.
60. Coll, M., Frederick, C. A., Wang, A. H., and Rich, A. (1987) *Proc. Natl. Acad. Sci. U.S.A. 84*, 8385−8389.
61. Alexeev, D. G., Lipanov, A. A., and Skuratovski, I. Ya. (1987) *Nature 325*, 821−823.
62. Park, H.-S., Arnott, S., Chandrasekaran, R., Millane, R. P., and Campagnari, F. (1987) *J. Mol. Biol. 197*, 513−523.
63. Kuga, S. (1981) *J. Chromatogr. Sci. 206*, 449−461.
64. Zimmerberg, J., and Parsegian, V. A. (1986) *Nature 323*, 36−39.
65. Bezrukov, S. M., Vodyanoy, I., and Parsegian, V. A. (1994) *Nature 370*, 279−281.

BI9820154